APPLIED AND ENVIRONMENTAL MICROBIOLOGY, Aug. 2002, p. 4067–4073 Vol. 68, No. 8
0099-2240/02/$04.00+0 DOI: 10.1128/AEM.68.8.4067–4073.2002


# Exploration of Inorganic C and N Assimilation by Soil Microbes with Time-of-Flight Secondary Ion Mass Spectrometry†

John B. Cliff,[1]* Daniel J. Gaspar,[2] Peter J. Bottomley,[1] and David D. Myrold[1]

*Department of Crop and Soil Science, Oregon State University, Corvallis, Oregon 97331-7306,[1] and William R. Wiley Environmental and Molecular Sciences Laboratory, Pacific Northwest National Laboratory, Richland, Washington 99352[2]*

Received 28 December 2001/Accepted 25 April 2002

**Stable C and N isotopes have long been used to examine properties of various C and N cycling processes in soils. Unfortunately, relatively large sample sizes are needed for accurate gas phase isotope ratio mass spectrometric analysis. This limitation has prevented researchers from addressing C and N cycling issues on microbially meaningful scales. Here we explored the use of time-of-flight secondary ion mass spectrometry (TOF-SIMS) to detect $^{13}C$ and $^{15}N$ assimilation by individual bacterial cells and to quantify N isotope ratios in bacterial samples and individual fungal hyphae. This was accomplished by measuring the relative abundances of mass 26 ($^{12}C^{14}N^-$) and mass 27 ($^{13}C^{14}N^-$ and $^{12}C^{15}N^-$) ions sputtered with a $Ga^+$ probe from cells adhered to an Si contact slide. TOF-SIMS was successfully used to locate and quantify the relative $^{15}N$ contents of individual hyphae that grew onto Si contact slides in intimate contact with a model organomineral porous matrix composed of kaolin, straw fragments, and freshly deposited manure that was supplemented with $^{15}NO_3^-$. We observed that the $^{15}N$ content of fungal hyphae grown on the slides was significantly lower in regions where the hyphae were influenced by N-rich manure than in regions influenced by N-deficient straw. This effect occurred over distances of tens to hundreds of microns. Our data illustrate that TOF-SIMS has the potential to locate N-assimilating microorganisms in soil and to quantify the $^{15}N$ content of cells that have assimilated $^{15}N$-labeled mineral N and shows promise as a tool with which to explore the factors controlling microsite heterogeneities in soil.**

During the past 15 years, use of the stable isotopes $^{13}C$ and $^{15}N$ combined with isotope ratio mass spectrometry has fueled insightful research into N and C cycling in soils (4). For instance, studies have shown that high rates of both $NH_4^+$ and $NO_3^-$ assimilation can coexist in the same soil volume (9, 10, 27) despite the fact that $NO_3^-$ assimilation is repressed by the presence of $NH_4^+$ (2, 26, 31). This apparent anomaly has been hypothesized to result from microsite heterogeneities that permit the simultaneous assimilation of $NO_3^-$ and $NH_4^+$ (9, 10, 27). In theory, labeling studies with $^{15}N$ could be used to examine this microsite hypothesis. Unfortunately, the relatively large sample size required to analyze $^{15}N$ by standard gas phase isotope ratio mass spectrometry has stymied this approach.

The use of radioactive isotopes is one way to circumvent the sample size limitations imposed by standard mass spectrometry methods. For example, direct observation of microbial C assimilation by individual microbial cells in environmental samples has been illustrated by using autoradiographic techniques (7, 14). Although $^{13}N$ has been used as a powerful tool with which to elucidate reaction mechanisms (2), its relatively short half-life (9.96 min) (21) precludes its use for environmental studies, such as N assimilation by individual cells. Time-of-flight secondary ion mass spectrometry (TOF-SIMS) (1, 32) has the potential to alleviate the problem of sample size when stable isotopes are used and thereby enable microbial metabolism to be studied on submillimeter scales.

In TOF-SIMS, a pulsed primary ion beam bombards a sample surface. When the primary ion impacts the surface, secondary electrons, negative and positive ions, and neutral species are sputtered into the gas phase. The extracted ions are accelerated to equal kinetic energies before traveling through a long flight tube to a detector. Thus, the time from primary ion impact to detection is proportional to $(m/z)^{1/2}$. Rastering of the primary beam allows spatial imaging, and region-of-interest analysis enables acquisition of mass spectra of specific areas of the sample. Secondary electrons may be collected to form a secondary electron image.

Recently, $^{13}C$-to-$^{12}C$ isotope ratio analyses of archaeal-bacterial consortia by SIMS analysis of sputtered $C_2^-$ ions has been reported (23). Because of low ionization yields, however, direct evaluation of $^{15}N$-to-$^{14}N$ ratios is not practical. Negative secondary ion yield due to primary ion sputtering is positively correlated with electron affinity of the secondary fragment of interest (22). Thus, because of their extremely high electron affinity (3.9 eV) (5), the yield of $CN^-$ ions is particularly high. This phenomenon is serendipitous for scientists studying C and N assimilation in biological materials (8, 15, 16, 20) but has not been capitalized upon for studying single microbial cells. Because of the potential for high spatial resolution and excellent detection limits for the $CN^-$ isotopes, TOF-SIMS has the potential to be a powerful tool for the exploration of C and N cycling on microbially meaningful scales in environmental systems.

Our work has focused on the development of TOF-SIMS to study C and N assimilation on a microbial scale and to explore

* Corresponding author. Mailing address: Department of Crop and Soil Science, 3017 Agriculture and Life Sciences Building, Oregon State University, Corvallis, OR 97331-7306. Phone: (541) 737-9299. Fax: (541) 737-5737. E-mail: John.Cliff@orst.edu.

† Oregon Agricultural Experiment Station technical paper 11812.

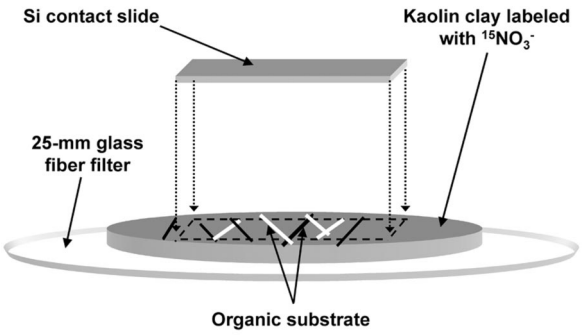


FIG. 1. Schematic representation of a model soil system used to study $NH_4^+$ and $NO_3^-$ assimilation in fungal hyphae. Pieces of straw and manure were placed on kaolin with 1 mM $^{15}NO_3^-$ added, covered with an Si contact slide, and incubated for 5 days.

the factors that control N assimilation on a submillimeter scale in soils. We report the preliminary results of this work here.

## MATERIALS AND METHODS

**Bacterial species and growth conditions.** *Pseudomonas fluorescens* strain HK44 (19) and the $NH_3$-oxidizing autotroph *Nitrosomonas europaea* (ATCC 19178) were used in these studies. *P. fluorescens* was grown in an adaptation of Hoagland's mineral medium (pH 7) (17) containing glucose (11 mM) and either 3.3 mM $(NH_4)_2SO_4$ or 6.6 mM $KNO_3$ at defined atom percent $^{15}N$ values. The medium was either filter sterilized through 0.22-μm-pore-size polycarbonate filters prior to use, or the N sources and the remainder of the medium were autoclaved separately and combined prior to inoculation. *P. fluorescens* was grown on an orbital shaker at 150 rpm at 23°C in the dark for 72 h. Cells were harvested by centrifugation and washed three times in 20 ml of 0.1 M phosphate buffer (pH 7) and five times in distilled deionized $H_2O$. Killed control samples of *P. fluorescens* were prepared by UV irradiation of liquid cultures.

*N. europaea* was grown in a variation of the medium reported by Duddleston et al. (11) containing isotopically defined C and N sources. In our medium, the carbonate buffer was omitted and C was supplied in the headspace as either natural-abundance $CO_2$ derived from acidifying $NaHCO_3$ or as $^{13}CO_2$ produced from 98 atom% $NaH^{13}CO_3$. Ammonium (50 mM N) was added as natural-abundance $(NH_4)_2SO_4$ or as 99 atom% $(^{15}NH_4)_2SO_4$. Growth was carried out in a 1-liter Erlenmeyer flask containing 300 ml of medium. The flask was sealed with a bored butyl stopper attached to an anaerobic culture tube (Bellco Glass, Inc., Vineland, N.J.) in which a 1/8-in.-diameter hole was drilled in the side to allow gas exchange with the culture headspace. The reservoir contained 1.0 mmol of isotopically defined $NaHCO_3$. The medium was cooled under $N_2$ to limit entry of atmospheric $CO_2$, 350 ml of $N_2$ was replaced with $O_2$, and 2 ml of 1 M HCl was added to the $NaHCO_3$ in the reservoir to produced natural-abundance $CO_2$ or 98 atom% $^{13}CO_2$. Cultures were grown at 27°C on an orbital shaker at 150 rpm in the dark until they reached an optical density at 600 nm of >0.1. Cells were harvested as described for *P. fluorescens*.

**Bacterial analyses.** Bulk samples of bacterial cells for high-mass-resolution analysis were grown as described above, fixed with formalin (2% final concentration), smeared onto Si slides cut from Si wafers 100 mm in diameter by 0.5 mm thick (United States Semiconductor, Lee's Summit, Mo.), and allowed to dry. For spatial imaging, bacterial cells were fixed with formalin and stained with 4′,6′-diamidino-2-phenylindole (DAPI) as described elsewhere (3). Stained cells were washed three additional times in distilled, deionized $H_2O$ before analysis. Aliquots (10 μl) of a cell suspension containing about $10^4$ cells were pipetted onto Si wafers and allowed to dry in the dark.

**Model soil systems (mineral-organic interfaces).** A simple model system was used to examine the assimilation of $NH_4^+$ and $NO_3^-$ by fungi associated with mineral surfaces. A portion (0.25 g) of well-crystallized kaolin clay (30) was suspended in $H_2O$ and filtered onto a glass fiber filter to produce a 15-mm-diameter cylinder of clay (Fig. 1). The clay was labeled with 0.25 ml of 1 mM, 99 atom% $^{15}NO_3^-$; organic substrates (straw and fresh dairy manure) were placed on the clay; and the assembly was covered with an Si contact slide. The assembly was placed in a glass container, covered with aluminum foil to limit evaporation, incubated for 5 days, and processed for TOF-SIMS analysis as described below.

**Native soil system.** An Si contact slide was buried in a clay soil of a riparian area. Ryegrass seeds were planted around the slide, and 2 weeks later 10 ml of 99 atom% $(^{15}NH_4^+)_2SO_4$ (1 mM N) and 10 ml of 1 mM natural-abundance $KNO_3^-$ were injected into the soil in the vicinity of the slide. After 5 days, the Si slide was removed and processed for TOF-SIMS analysis as described below. Killed controls were prepared by gamma irradiating 20-$cm^3$ soil cores at a dose of 2 megarads.

**TOF-SIMS analyses.** TOF-SIMS was performed by using a Physical Electronics International TRIFT-II instrument (Physical Electronics International, Eden Prairie, Minn.). Analytical conditions can be optimized either for a mass resolution (mass divided by the difference in mass) of greater than 9,000 or a spatial resolution of less than 200 nm. The ion beam may be used in continuous DC mode to erode the surface of the target of interest in a process known as sputtering. For high mass resolution analysis, an electrodynamically bunched 15-keV, 600-pA $Ga^+$ beam (<1-ns temporal pulse width after bunching) was used. The samples were sputtered at a dose of 3.6 pA $\mu m^{-2}$, and areas of 50 by 50 μm were analyzed. For high spatial resolution analysis, a 25-keV, 60-pA $Ga^+$ beam with a 17-ns temporal pulse width was used. The secondary electron detector was used with the ion gun in continuous DC mode to locate specific bacteria and fungal hyphae. Samples used to produce ion images of individual bacteria were sputtered at a dose of about 4 pA $\mu m^{-2}$. The sputter doses used in our analyses were sufficient to remove adventitious C (6) as a potential source of isobaric interference (Fig. 2).

**Isotope ratio analyses.** Isotope ratio analyses of bulk bacterial standards, and of model and native soil systems, were performed in high-spatial-resolution mode. We tested the ability of TOF-SIMS to quantify organic N isotope ratios by using samples of *P. fluorescens* grown in six isotopically defined N sources ranging from natural-abundance to approximately 50-atom% $^{15}N$. Standards were sputtered, and areas of 50 by 50 μm were analyzed until the mass 27 signal equaled ≥5,000 counts.

To estimate the atoms percent $^{15}N$ in the fungal hyphae of model soil systems, the secondary electron detector was used to initially locate the specimen, which was sputtered at a dose of 2.4 pA $\mu m^{-2}$. Ion images were collected, and a region of interest containing hyphae was defined. Isotope ratio data were collected until the sum of the mass 26 and mass 27 peaks was ≥2,500 ion counts. The entire process generally took less than 5 min per analysis.

Ion images of the native soil system were collected as described above, except that the images were collected for 10 min.

Atoms percent $^{15}N$ in the target samples was estimated by using the following equation:

$$^{15}N\% = \frac{^{27}CN^{-*}}{^{26}CN^- + ^{27}CN^{-*}} \quad (1)$$

where $^{15}N\%$ represents the atoms percent $^{15}N$, $^{26}CN^-$ is the total ion count at mass 26, and $^{27}CN^{-*}$ is the adjusted ion count at mass 27. Here, $^{27}CN^-$ has been adjusted for the presence of natural-abundance $^{13}C$ (1.1 atom% $^{13}C$) by using the equation $^{27}CN^{-*} = {}^{27}CN^- - 0.011{}^{26}CN^-$, where $^{27}CN^-$ represents the total unadjusted ion counts at mass 27.

## RESULTS

**Abiotic N assimilation.** Control samples of *P. fluorescens* killed with UV radiation in liquid culture showed no assimilation of either $^{15}NH_4^+$ or $^{15}NO_3^-$ after 48 h (data not shown). Organic $^{15}N$ contents (atoms percent) of gamma-irradiated soils were not significantly different from those of soils labeled with natural-abundance $NH_4^+$ ($\alpha = 0.05$) but were significantly lower than those of live soils labeled with $^{15}NH_4^+$ ($\alpha = 0.05$).

**C and N assimilation.** Figure 3 compares partial TOF-SIMS mass spectra of *P. fluorescens* cells grown with either natural-abundance $NH_4^+$ or 99 atom% $^{15}NH_4^+$ as the sole N source. TOF-SIMS was successful in detecting N in bacterial smears, as shown by the large $^{26}CN^-$-to-$^{27}CN^-$ ratio of samples of bacteria grown in natural-abundance $NH_4^+$ and the large $^{27}CN^-$-to-$^{26}CN^-$ ratio of samples grown in $^{15}NH_4^+$. Similarly, TOF-SIMS was able to detect $NH_4^+$ assimilation in the gram-positive bacterium *Bacillus subtilis* and in the basidiomycete

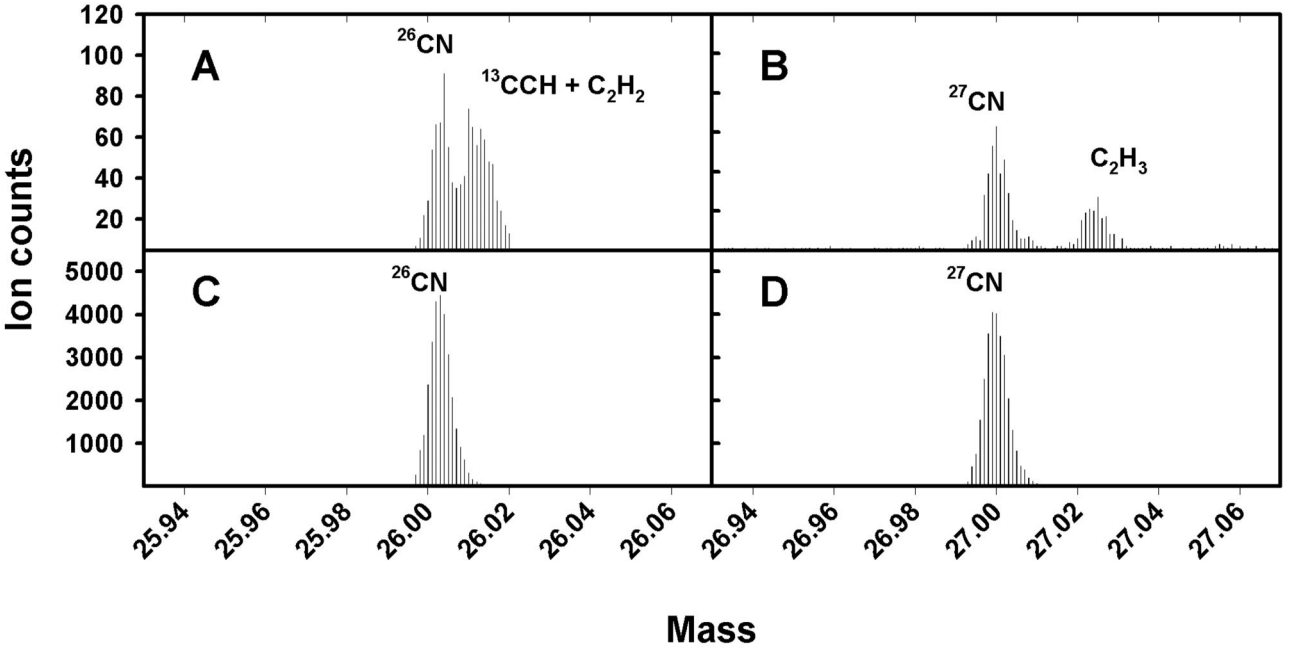


FIG. 2. Partial high-mass-resolution spectra of smears of *P. fluorescens* before (A and B) and after (C and D) sputtering, showing the elimination of isobaric signals from adventitious C. Note the scale on the *y* axis.

*Pleurotis ostreatus* (data not shown). We also detected $NO_3^-$ assimilation in *P. fluorescens* grown with labeled $^{15}NO_3^-$ as the sole N source (data not shown).

TOF-SIMS detected assimilation of both C and N in the gram-negative autotroph *N. europaea*, as illustrated by the shift in the primary $CN^-$ isotope peaks in samples labeled with different C and N isotopes (Fig. 4). Theoretically, the TRIFT-II instrument is capable of a mass resolution (mass divided by the change in mass) of greater than 9,000 (about 0.003 atomic mass unit at mass 27); however, because of charging effects and sample roughness, we were unable to differentiate reliably between $^{13}C^{14}N^-$ and $^{12}C^{15}N^-$ despite the fact that a theoretical mass resolution of only 4,500 is needed to separate these peaks.

**Single-cell detection.** Figure 5 shows a comparison of $^{26}CN^-$ (red), $^{27}CN^-$ (green), and $^{28}CN^-$ (white) ion images with

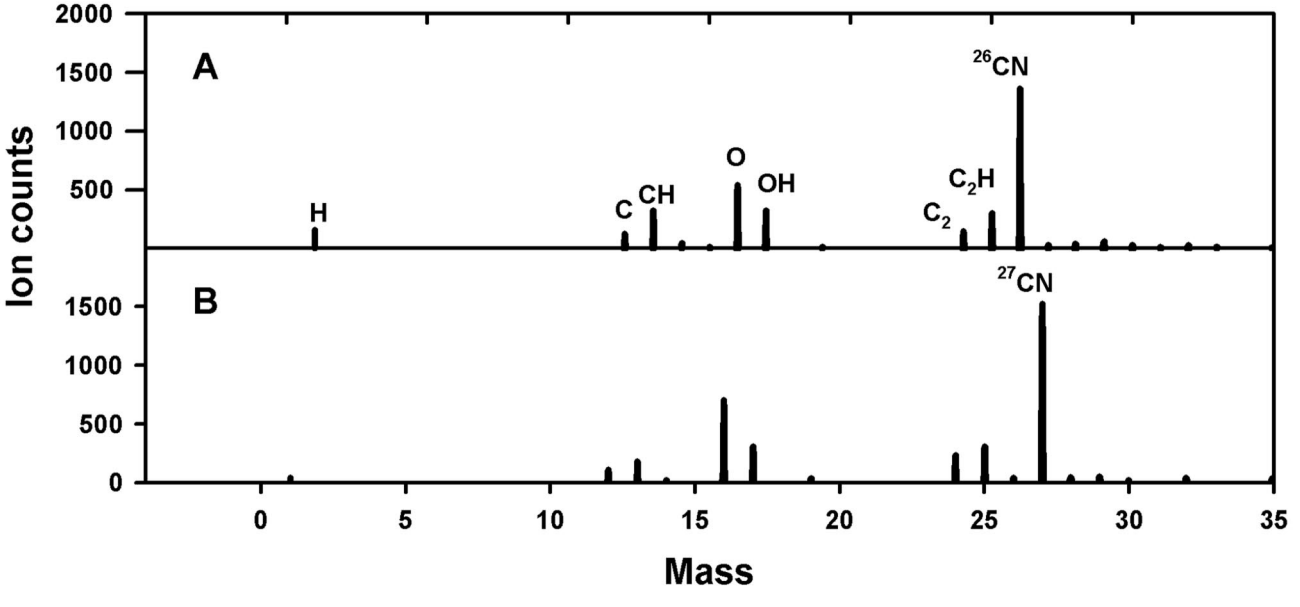


FIG. 3. Comparison of partial negative TOF-SIMS spectra of smears of *P. fluorescens* grown with natural-abundance $NH_4^+$ (A) or 99 atom% $^{15}NH_4^+$ (B) as the sole N source.

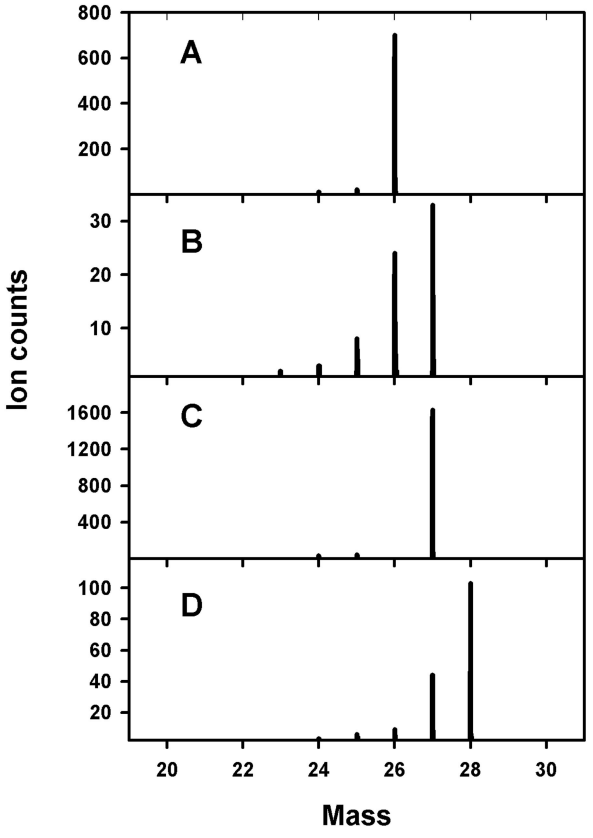


FIG. 4. Comparison of partial negative TOF-SIMS spectra of smears of *N. europaea* grown with $^{12}CO_2$ and $^{14}NH_4^+$ (A), $^{13}CO_2$ and $^{14}NH_4^+$ (B), $^{12}CO_2$ and $^{15}NH_4^+$ (C), or $^{13}CO_2$ and $^{15}NH_4^+$ (D) as the sole C and N sources.

DAPI epifluorescence images of *N. europaea* cells grown with 98 atom% $^{13}CO_2$ as the primary C source and 99 atom% $^{15}NH_4^+$ as the sole N and energy source. All three ion images overlapped the epifluorescent image. The significant mass 28 ion count indicates that the organisms assimilated both $^{13}C$ and $^{15}N$. The diffuse background signal observed for mass 28 is likely from $Si^-$ ions. We believe that the presence of $^{26}CN^-$ and $^{27}CN^-$ ions is an indication of contamination by ambient $CO_2$.

**Isotope ratio standards.** We found that it was necessary to correct for the contribution of $^{13}C^{14}N^-$ ions to the mass 27 signal by using equation 1 (not doing so resulted in about threefold overestimation of the $^{15}N$ content [atoms percent] at natural abundance). With this correction, TOF-SIMS was successful in quantifying the $^{15}N$ content of bacterial standards with a wide range of $^{15}N$ values (atoms percent; $r^2 > 0.999$; data not shown). Relative errors between theoretical and measured $^{15}N$ values ranged between $-2.7$ and $-6.1\%$; e.g., the 40 atom% samples averaged 37.4 atom% $\pm$ 0.25 atom% (99% confidence interval [CI]), a relative difference of $-6.1\%$.

**Model systems.** We used the region-of-interest capabilities of TOF-SIMS to explore inorganic N assimilation by fungal hyphae in a model clay-organic matrix and in soil. Figure 6A shows a secondary electron image of an Si contact slide that had been in contact with a straw-manure interface associated with kaolin clay labeled with 1 mM $^{15}NO_3^-$. Electron-poor sputtered areas measuring 55 by 55 μm are clearly visible. Figure 6B shows a corresponding light micrograph in which the approximate $^{15}N$ content (atoms percent) of the hyphal wall was estimated from 50-μm-long region-of-interest analyses of the hyphae. In this instance, the straw was overlain by the manure and the isotopic composition of the hyphae changed from about 20 to about 10 atom% $^{15}N$ over a distance of 40 μm. Figure 6C shows another microsite interface on the same contact slide within a linear distance of 300 μm from the hyphae pictured in Fig. 6B. A single hypha in a soil pore changes from 20 to about 10 atom% $^{15}N$ as it approaches the manure interface and over a distance of about 200 μm.

**Native soil system.** We used the $SiO_2^-$ ion as an indicator of inorganic soil particles, as sputtering removed most of the surface oxidation from our Si contact slides and clay minerals did not yield significant $Al^-$ ions under the circumstances of these analyses. The distribution of $SiO_2^-$ ions (yellow) and the sum of $^{26}CN^-$ and $^{27}CN^-$ ions (blue; an indicator of organic matter) are shown in Fig. 7A. Inorganic particles seem to be distributed in a diffuse, random pattern, whereas there are five distinct clusters of organic materials, three of which have the rod-shaped morphology of bacteria. The putative, rod-shaped bacteria all assimilated $^{15}N$ as shown by high $^{27}CN^-$ signals and were estimated to range from 9 to 38 atom% $^{15}N$ (Fig. 7B). The other pieces of organic matter did not show incorporation of $^{15}N$ (Fig. 7B). A second, nearby section of the contact slide shows a bacterium more strongly labeled with $^{15}N$ (39 atom% $\pm$ 4 atom% $^{15}N$ [99% CI]) than an adjacent fungal hypha (6.3 atom% $\pm$ 0.2 atom% $^{15}N$ [99% CI]), despite the fact that the organisms are separated by less than 15 μm (Fig. 7C).

FIG. 5. Comparisons of an epifluorescence image (A) and $^{26}CN^-$ (B), $^{27}CN^-$ (C), and $^{28}CN^-$ (D) ion images of DAPI-stained *N. europaea* cells grown with 99 atom% $^{15}NH_4^+$ as the sole N and energy source and 98 atom% $^{13}CO_2$ as the sole C source. Bar, 10 μm.

FIG. 6. Secondary electron image (A) and light micrographs (B and C) of Si contact slides that were in contact with a model soil system. The system consisted of a straw-manure interface on kaolinite to which $^{15}NO_3^-$ was added. The area in panel A is bracketed in yellow in panel B. Dark, electron-poor sputtered areas in panel A are represented by white boxes in panel B. The values adjacent to the analysis areas are the $^{15}N$ contents (atoms percent) of the region of interest of the fungal hyphae (shaded red). The dashed line represents the straw-manure interface. (C) Light micrograph of an Si contact slide illustrating microsite heterogeneity of differential $^{15}N$ assimilation by fungal hyphae growing across a model soil microsite. The arrangement is similar to that of panel B, except that the dashed line represents the straw boundary and the manure boundary is about 10 μm left of and parallel to the panel boundary. Bars, 100 μm.

FIG. 7. Secondary ion images of an Si contact slide from a clay riparian soil. The soil was labeled with 1 mM $^{15}NH_4^+$ and 1 mM $NO_3^-$. (A) Yellow represents $SiO_2^-$, an indicator of the presence of inorganic soil particles; blue represents the sum of the $^{26}CN^-$ and $^{27}CN^-$ ion counts, an indicator of organic matter. Bar, 1.7 μm. (B) The same image as in panel A, except that red represents $^{26}CN^-$ and green represents $^{27}CN^-$, showing the assimilation of $^{15}N$ by the putative rod-shaped bacteria. (C) A nearby image showing a fungal hypha and a bacterium; red represents $^{26}CN^-$, and green represents $^{27}CN^-$. Bar, 2.5 μm.

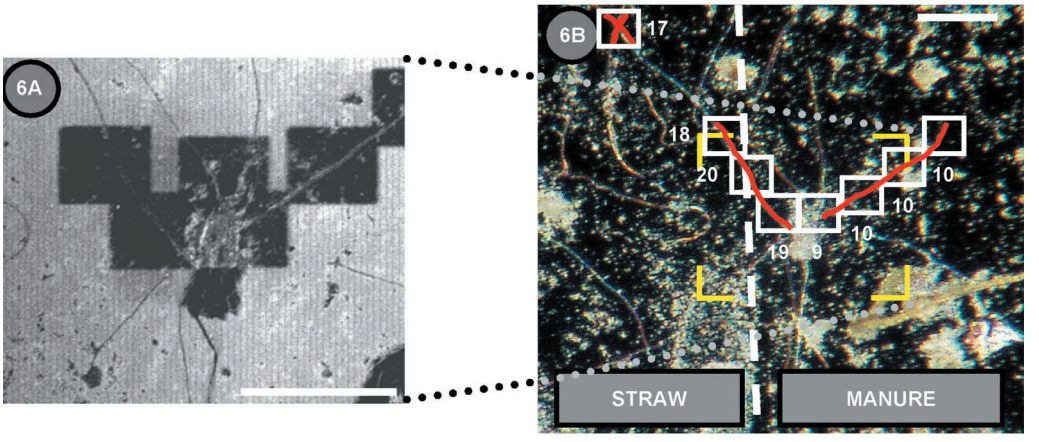
6A
6B
17
18
20
10
10
10
19
9
STRAW
MANURE

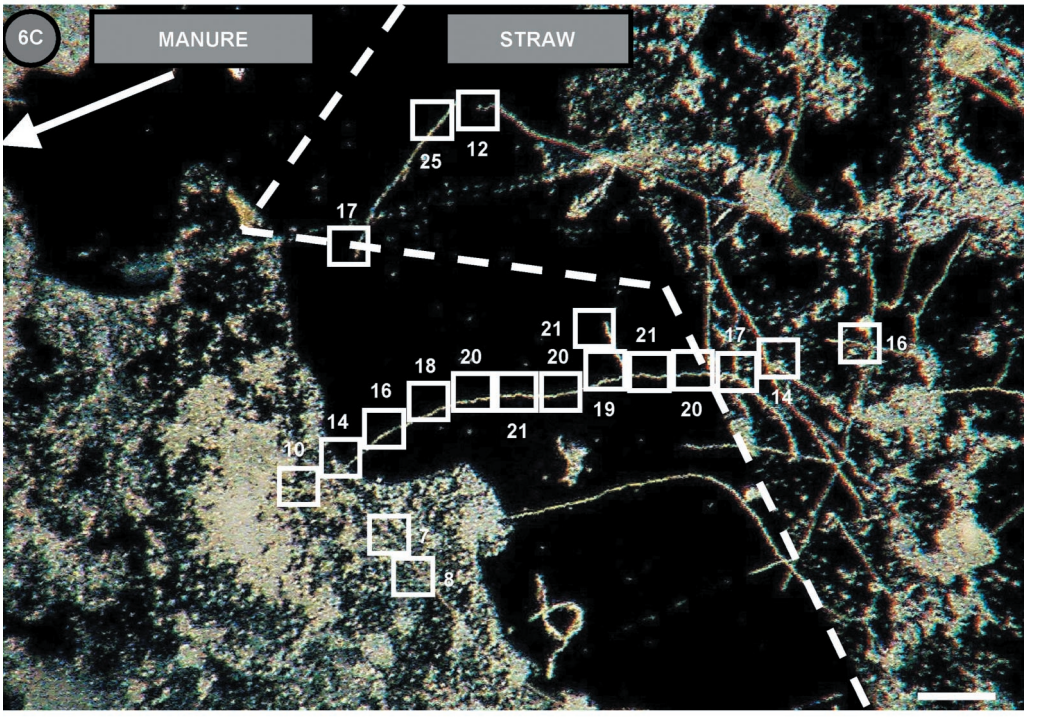
6C
MANURE
STRAW
25
12
17
21
21
17
16
18
20
20
16
19
20
14
14
21
10
7
8

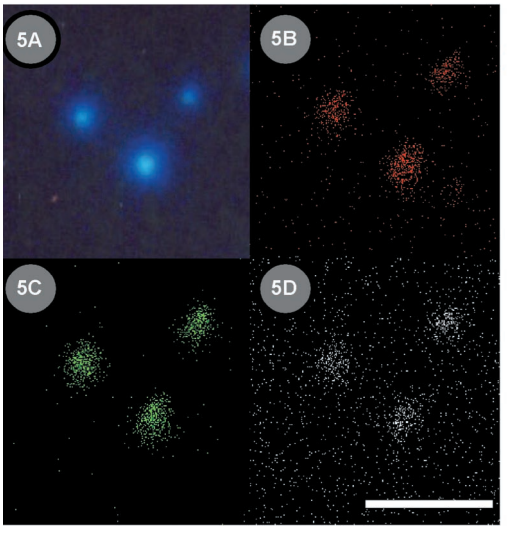
5A
5B
5C
5D

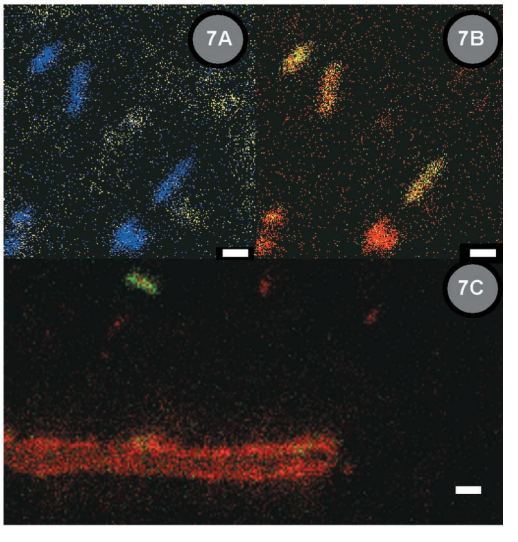
7A
7B
7C

## DISCUSSION

There are several important considerations that must be addressed if isotope ratio N assimilation measurement data are to be acquired from secondary ion images of microbes, including clear delineation of the target and determination of the limits of precision and accuracy.

The overlapping images obtained from epifluorescence microscopy and TOF-SIMS (Fig. 5) illustrated that the 200-nm spatial resolution of the TRIFT-II instrument is sufficient to resolve C and N assimilation in individual bacterial cells. Secondary ion images clearly delineated fungal hyphae as well.

Microbial target delineation requires not only high two-dimensional spatial resolution but also an estimate of the depth of sampling to ensure that cellular components, and not surface contaminants, have been analyzed. On the basis of empirically derived sputter rates of Si-$SiO_2$ standards and a conservative assumption of a sputter rate for C of about 25% of that for Si (28), we sputtered about 4 Å of fungal material away prior to region-of-interest analysis. Assuming that a single atomic layer is about 2 Å, an average of two atomic layers were removed. Therefore, only the very outside of the target was analyzed. This may be of importance, for example, in ascertaining if the assimilated $^{15}N$ was associated with exterior cellular proteins, cell wall constituents, or cytoplasm.

We cannot completely discount the possibility that the observed difference in the atom percent $^{15}N$ signature of the hyphae in Fig. 6 was an artifact of organic material in contact with the fungal hyphae. If this were the case, however, we would expect to see greater variability in the $^{15}N$ signature on the same side of an interface of two substrates. Furthermore, there was a change in the apparent fungal $^{15}N$ signature shown in Fig. 6C despite the fact that the hypha seemed to be growing across a void. Thus, we were measuring primarily the isotopic signature of the microbial cells we targeted rather than contaminating organic matter.

The accuracy and precision of SIMS analysis are limited by several factors, which include primary beam stability, matrix effects, sample charging, and imprecision due to the random nature of secondary ion emission (13). Accuracy also depends upon being able to discriminate among isobaric species.

For high spatial resolution analyses, we used a primary ion pulse width of 17 ns, which effectively reduced mass resolution to 1 atomic mass unit. The sputtering doses we used eliminated isobaric interferences from adventitious C (Fig. 2), which allowed us to correct solely for the isobaric interference of $^{13}C^{14}N^-$ with $^{12}C^{15}N^-$ in the mass 27 peak by using equation 1.

Our analysis of bacterial cells with known amounts (atoms percent) of $^{15}N$ provided a measurement of the accuracy of TOF-SIMS for isotopic analysis. The *y* intercept (0.12) of the linear regression line fitted to the measured versus theoretical $^{15}N$ data (atoms percent) was not significantly different from 0 ($\alpha = 0.05$); however, the slope (0.95) of the regression line was significantly less than 1 ($\alpha = 0.05$), which resulted in underestimates of the isotopic composition. We do not know the cause of this systematic error for enriched samples; nevertheless, our results suggest that TOF-SIMS can measure the isotopic composition of organic samples with a relative accuracy of 6% or better.

Secondary ion emissions conform to a Poisson probability distribution; therefore, precision is a function of the number of ion counts collected. On the basis of the work of Fitzsimmons et al. (13), we estimated the standard deviations of our isotope ratio measurements. For calculations of $^{15}N$ content (atoms percent), the estimated standard deviation ( $\hat{s}_{15_N}$ ) of a measurement is given by the equation

$$\hat{s}_{15_N} \approx \sqrt{\frac{^{27}CN^{-} * {}^{26}CN^{-}}{[^{27}CN^{-} * + {}^{26}CN^{-}]^3}} \quad (2)$$

If we further assume that, given enough ion counts, the Poisson distribution approximates a Gaussian one (13), we can put 99% CIs on the estimated $^{15}N$ values (atoms percent) in Fig. 6 and 7. The results of this analysis indicate that all of the $^{15}N$ data presented in Fig. 6 have a theoretical 99% CI of $\leq \pm 1.2$ atom%. The data comprising the standard curve had 99% CIs ranged between $\pm 0.07$ atom% $^{15}N$ for the natural-abundance samples and $\pm 0.50$ atom% $^{15}N$ for the 48-atom% $^{15}N$ samples. Thus, TOF-SIMS was capable of providing adequate precision for determination of the isotopic composition of bacterial cells and fungal hyphae (Fig. 7) and allowed us to separate the relative differences in $^{15}N$ content (atoms percent) across microsite boundaries (Fig. 6).

The $^{15}N$ abundances of the fungal hyphae analyzed were lower in areas associated with manure than in areas associated with straw (Fig. 6), and this may be explained by several biological hypotheses. The relative abundance of $NH_4^+$ may have been higher under the manure interface because of mineralization of organic N contained in the manure or because of higher rates of denitrification. Manure typically has a low C/N ratio, allowing net mineralization of organic N (12, 25, 29). A greater contribution of natural-abundance $NH_4^+$ mineralizing from the manure would decrease the value of the $^{15}N$ signature. Microsite heterogeneity of denitrifying activity due to organic hot spots has been observed before (18, 24). Loss of $^{15}NO_3^-$ due to denitrification would increase the relative proportion of natural-abundance $NH_4^+$ locally available for assimilation and lower the value of the $^{15}N$ signature. Similarly, the causes of the significant differences in microbial $^{15}NH_4^+$ assimilation we observed in native soil systems are not known and require additional study (Fig. 7). Nevertheless, these experiments illustrate the potential to utilize this technology to study the influence of microsite heterogeneity on N cycling in natural soil systems.

**Conclusions.** We have shown that TOF-SIMS is capable of detecting C and N assimilation in individual bacterial and fungal cells. The method has potential to be used to study N assimilation on a submillimeter scale in soils. The combined qualities of high spatial resolution, low detection limits, and short analysis time makes TOF-SIMS analysis a potentially powerful tool with which to study C assimilation on small scales as well. The quality of isotope ratio data is constrained by Poisson counting statistics and thus analysis time. Therefore, long analysis times would be required to achieve high-precision isotope ratio measurements, particularly in natural-abundance samples. TOF-SIMS, however, offers the possibility of using stable C and N isotopes to spatially resolve patterns of C and N assimilation on a submillimeter scale in environmental samples. Acceptable theoretical precision for 50-μm

lengths of $^{15}$N-labeled fungal hyphae in our model systems was achieved with analysis times of less than 5 min. Current research directions include calibration of sputter rates of microbial cells to better define sampling depth and use of TOF-SIMS to understand the mechanisms that lead to, and the spatial scale of, soil N assimilation microsites.

## ACKNOWLEDGMENTS

A portion of this work was funded through U.S. Department of Agriculture Cooperative State Research, Education, and Extension Service National Research Institute grant NRI97-35107-4357. TOF-SIMS analysis was performed at the W. R. Wiley Environmental Molecular Sciences Laboratory, a national scientific user facility sponsored by the U.S. Department of Energy's Office of Biological and Environmental Research and located at the Pacific Northwest National Laboratory (PNNL). PNNL is operated for the U.S. Department of Energy by Battelle.

Thanks go to Al Soeldner for insightful discussions concerning sample preparation and to Mark Engelhard for help with preliminary work.

## REFERENCES

1. **Benninghoven, A., F. G. Rüdenauer, and H. W. Werner.** 1987. Secondary ion mass spectrometry: basic concepts, instrumental aspects, applications and trends. John Wiley & Sons, Inc., New York, N.Y.
2. **Betlach, M. R., J. M. Tiedje, and R. B. Firestone.** 1981. Assimilatory nitrate uptake in *Pseudomonas fluorescens* studied using nitrogen-13. Arch. Microbiol. **129:**135–140.
3. **Bottomley, P. J.** 1994. Light microscopic methods for studying soil microorganisms, p. 81–105. *In* R. W. Weaver, S. Angle, P. Bottomley, D. Bezdicek, S. Smith, A. Tabatabai, A. Wollum, S. H. Mickelson, and J. M. Bigham. (ed.), Methods of soil analysis, part 2: microbiological and biochemical properties. Soil Science Society of America, Madison, Wis.
4. **Boutton, T. W., and S.-I. Yamasaki.** 1996. Mass spectrometry of soils. Marcel Dekker, Inc., New York, N.Y.
5. **Bradforth, S. E., E. H. Kim, D. W. Arnold, and D. M. Neumark.** 1993. Photoelectron spectroscopy of CN-, NCO-, and NCS-. J. Chem. Phys. **98:** 800–810.
6. **Briggs, D., and M. P. Seah.** 1990. Practical surface analysis. John Wiley & Sons, Inc., New York, N.Y.
7. **Brock, M. L., and T. D. Brock.** 1968. The application of micro-autoradiographic techniques to ecological studies. Mitt. Int. Ver. Limnol. **15:**1–31.
8. **Chandra, S., D. R. Smith, and G. H. Morrison.** 2000. Subcellular imaging by dynamic SIMS ion microscopy. Anal. Chem. **72:**104A–114A.
9. **Chen, J., and J. M. Stark.** 2000. Plant species effects and carbon and nitrogen cycling in a sagebrush-crested wheatgrass soil. Soil Biol. Biochem. **32:**47–57.
10. **Davidson, E. A., J. M. Stark, and M. K. Firestone.** 1990. Microbial production and consumption of nitrate in an annual grassland. Ecology **71:**1968–1975.
11. **Duddleston, K. N., P. J. Bottomley, A. Porter, and D. J. Arp.** 2000. Effects of soil and water content on methyl bromide oxidation by the ammonia-oxidizing bacterium *Nitrosomonas europaea*. Appl. Environ. Microbiol. **66:**2636–2640.
12. **Eghball, B.** 1999. Nitrogen mineralization from field-applied beef cattle feedlot manure or compost. Soil Sci. Soc. Am. J. **64:**2024–2030.
13. **Fitzsimmons, I. C. W., B. Harte, and R. M. Clark.** 2000. SIMS stable isotope measurement: counting statistics and analytical precision. Miner. Mag. **64:** 59–83.
14. **Fliermans, C. B., and E. L. Schmidt.** 1975. Autoradiography and immunofluorescence combined for autoecological study of single cell activity with *Nitrobacter* as a model system. Appl. Environ. Microbiol. **30:**676–684.
15. **Gringon, N., S. Halpern, A. Gojon, and P. Fragu.** 1992. $^{14}$N and $^{15}$N imaging by SIMS microscopy in soybean leaves. Biol. Cell **74:**143–146.
16. **Hindie, E., B. Coulomb, and P. Galle.** 1992. SIMS microscopy: a tool to measure intracellular concentration of carbon 14-labeled molecules. Biol. Cell **74:**89–92.
17. **Hoagland, D. R., and D. I. Arnon.** 1950. The water culture method for growing plants without soil. Calif. Agric. Exp. Serv. Circ. 374.
18. **Højberg, O., N. P. Revsbech, and J. M. Tiedje.** 1994. Denitrification in soil aggregates analyzed with microsensors for nitrous oxide and oxygen. Soil. Sci. Soc. Am. J. **58:**1691–1698.
19. **King, J. M. H., P. M. DiGrazia, B. Applegate, R. Burlage, J. Sanseverino, P. Dunbar, F. Larimer, and G. S. Sayler.** 1990. Rapid, sensitive bioluminescent reporter technology for naphthalene exposure and biodegradation. Science **249:**778–781.
20. **Levy-Setti, R., and M. Le Beau.** 1992. Cytogenetic applications of high resolution secondary ion imaging microanalysis: detection and mapping of tracer isotopes in human chromosomes. Biol. Cell **74:**51–58.
21. **Meeks, J. C.** 1993. $^{13}$N techniques, p. 273–303. *In* R. Knowles and T. H. Blackburn (ed.), Nitrogen isotope techniques. Academic Press, San Diego, Calif.
22. **Odom, R. W.** 1993. Secondary ion mass spectrometry imaging, p. 345–394. *In* M. D. Morris (ed.), Microscopic and spectroscopic imaging of the chemical state. Marcel Decker, Inc., New York, N.Y.
23. **Orphan, V. J., C. H. House, K. Hinrichs, K. D. McKeegan, and E. F. DeLong.** 2001. Methane-consuming archaea revealed by directly coupled isotopic and phylogenetic analysis. Science **293:**484–487.
24. **Parkin, T. B.** 1987. Soil microsites as a source of denitrification variability. Soil Sci. Soc. Am. J. **51:**1194–1199.
25. **Pratt, P. F., F. E. Broadbent, and J. P. Martin.** 1973. Using organic wastes as nitrogen fertilizer. Calif. Agric. **27:**10–13.
26. **Rice, C. W., and J. M. Tiedje.** 1989. Regulation of nitrate assimilation by ammonium in soils and in isolated soil microorganisms. Soil Biol. Biochem. **21:**597–602.
27. **Schimel, J. P., and M. K. Firestone.** 1989. Nitrogen incorporation and flow through a coniferous forest soil profile. Soil Biol. Biochem. **53:**779–784.
28. **Seah, M. P.** 1981. Pure element sputter yields using 500–1000 eV argon ions. Thin Solid Films **81:**279–287.
29. **Smith, J. H., and J. R. Peterson.** 1982. Recycling nitrogen through land application of agricultural, food processing, and municipal wastes, p. 791–831. *In* F. J. Stevenson (ed.), Nitrogen in agricultural soils. American Society of Agronomy, Madison, Wis.
30. **Van Olphen, H., and J. J. Fripiat.** 1979. Data handbook for clay materials and other non-metallic minerals. Pergamon Press, Elmsford, N.Y.
31. **Van't Riet, J., A. H., Stouthammer, and R. J. Plant.** 1968. Regulation of nitrate assimilation and nitrate respiration in *Aerobacter aerogenes.* J. Bacteriol. **96:**1455–1464.
32. **Vickerman, J. C., A. Brown, and N. M. Reed.** 1989. Secondary ion mass spectrometry. Oxford University Press, New York, N.Y.